Global surface mass from a new combination of GRACE, modelled OBP and reprocessed GPS data

R. Rietbroek[a], M. Fritsche[b], S.-E. Brunnabend[c], I. Daras[d], J. Kusche[a], J. Schröter[c], F. Flechtner[d], R. Dietrich[b]

[a]*Institute of Geodesy and Geoinformation, Bonn University*
[b]*Institute for Planetary Geodesy, Dresden University of Technology*
[c]*Alfred Wegener Institute for Polar and Marine Research*
[d]*GFZ German Research Centre for Geosciences*

Abstract

Weekly surface loading variations are estimated from a joint least squares inversion of load-induced GPS site displacements, GRACE gravimetry and simulated ocean bottom pressure (OBP) from the Finite Element Sea-Ice Ocean model (FESOM).

In this study, we directly use normal equations derived from reprocessed GPS observations, where station and satellite positions are estimated simultaneously. The OBP weight of the model in the inversion is based on a new error model, obtained from 2 FESOM runs forced with different atmospheric data sets.

Our findings indicate that the geocenter motion derived from the inversion is smooth, with non-seasonal RMS values of 1.4, 0.9 and 1.9 mm for the X, Y and Z directions, respectively. The absolute magnitude of the seasonal geocenter motion varies annually between 2 and 4.5 mm. Important hydrological regions such as the Amazon, Australia, South-East Asia and Europe are mostly affected by the geocenter motion, with magnitudes of up to 2 cm, when expressed in equivalent water height.

The chosen solar radiation pressure model, used in the GPS processing, has only a marginal effect on the joint inversion results. Using the empirical CODE model slightly increases the annual amplitude of the Z component of the geocenter by 0.8 mm. However, in case of a GPS-only inversion, notable larger differences are found for the annual amplitude and phase estimates when applying the older physical ROCK models. Regardless of the used radiation pressure model the GPS network still exhibits maximum radial expansions in the order of 3 mm (0.45 ppb in terms of scale), which are most likely caused by remaining GPS technique errors.

In an additional experiment, we have used the joint inversion solution as a background loading model in the GPS normal equations. The reduced time series, compared to those without a priori loading model, show a consistent decrease in RMS. In terms of the annual height component, 151 of the 189 stations show a reduction of at least 10% in seasonal amplitude.

On the ocean floor, we find a positive overall correlation (0.51) of the inversion solution with time series from globally distributed independent bottom pressure recorders. Even after removing a seasonal fit we still find a correlation of 0.45. Furthermore, the geocenter motion has a significant effect on ocean bottom pressure as neglecting it causes the correlation to drop to 0.42.

Keywords: , Ocean bottom pressure, joint inversion, geocenter motion

1. Introduction

In the last decade, observations from increasingly dense geodetic GPS networks, and new satellite missions such as the Gravity Recovery and Climate Experiment, GRACE (Tapley et al., 2004), have shed light on global migration patterns of masses. The dynamic exchange of those masses between the ocean,

Email address: roelof@geod.uni-bonn.de (R. Rietbroek)

atmosphere, cryosphere and the terrestrial hydrosphere, are causing observable crustal deformations and perturbations in the orbits of satellites. The continued observation of those phenomena are crucial for our understanding of the system Earth.

However, measurement techniques come with their own shortcomings, making it attractive to combine multiple techniques to overcome this (Rietbroek et al., 2009; Wu et al., 2006; Kusche and Schrama, 2005). GRACE measures a global gravity field in weeks to months with resolutions in the order of several hundred km. Unfortunately, GRACE does not provide estimates of the important geocenter motion (i. e. the motion of the solid Earth w.r.t. the common center of mass of the Earth system, see Blewitt and Clarke (2003)). Furthermore, it yields unsufficiently accurate degree 2 Stokes coefficients (Chen et al., 2005) and is contaminated by strong anisotropic noise. On the other hand the GPS network only covers land and still contains only few sites in remote areas such as Africa and Antarctica. In addition, as deformation is the result of a damped convolution of surface loading, the GPS technique suffers from a decreased sensitivity to high resolution signal (van Dam et al., 2007). Over Europe, a comparison of the GPS site displacements with GRACE derived deformation has shown significant differences in the annual amplitude and phase (van Dam et al., 2007). The inconsistencies were mainly due to GPS technique errors and could not be explained by a realistic loading signal. As we will show later, using the reprocessing solution, we find a good consistency between low resolution surface loading from the inversion and the GPS site displacements.

Different approaches have been proposed to infer estimates of the surface mass variation from geodetic measurements of load-induced crustal deformation (Heflin and Watkins, 1999; Blewitt et al., 2001; Wu et al., 2002; Dong, 2003; Lavallée et al., 2006). Mostly, operational weekly Global Positioning System (GPS) solutions published by the International GNSS Service (IGS) have been applied to solve for the degree-1 spherical harmonics of the redistributed surface load. However, the results of Fritsche et al. (2009) demonstrate the impact of using reprocessed GPS observations on estimated low-degree spherical harmonics of the load. Their work concentrates on the differences in the estimated load parameters when applying a more sophisticated observation modelling strategy in the GPS data analysis. In particular, the consideration of higher-order ionospheric terms was found to reduce artificial variations in the time series of degree-1 coefficients during periods of a solar maximum. Moreover, the effects of a change in the radiation pressure modelling have been shown and discussed. Here, a significant reduction in geocenter amplitude of well known alias periods could be determined when applying a newer model for the effect of the radiation pressure acting on the GPS satellites.

A combination of GRACE release 1 gravity fields from CSR, GPS deformations and modelled OBP from the ECCO model has been studied before by Wu et al. (2006). They demonstrated the potential of the combination to simultaneously solve for low degree surface loading, geocenter motion and mitigate the effect of mass conservation of the ocean model. From a more theoretical approach, the effect of the GPS network geometry on the inversion has been discussed by Jansen et al. (2009).

In this study, we adapt the least squares inversion scheme of Rietbroek et al. (2009) to estimate weekly surface loading solutions up to spherical harmonic degree and order 30. Fed into the inversion are 1) the new TUD reprocessed GPS solution, 2) weekly GRACE GFZ-release 4 normal equations, 3) a priori ocean model information from FESOM (Timmermann et al., 2009) in the form of pseudo-observations with updated error-covariance (Brunnabend et al., 2010, submitted) and a modified observation equation.

Using our results, we elaborate on the magnitude and direction of the estimated geocenter, and compare the results with those of Rietbroek et al. (2009). Weekly Helmert parameters, revealing inconsistencies in the GPS network and processing, are estimated and quantified. The influence of the pressure radation model on the joint inversion solution has been studied. In a forward modelling experiment, we assess the consistency between the GPS data and the combination solution by propagating the joint inversion results to GPS station deformations. Furthermore, a comparison with time series from in-situ bottom pressure recorders (BPR) has been performed over the ocean.

2. Methodology

2.1. Joint inversion scheme

Our main objective is to estimate weekly sets of spherical harmonic coefficients, $T^{\sigma}_{nm}(t)$, of surface loading up to degree and order, n_{max}=30, which are linked to changes in the surface density $\Delta\sigma(\lambda,\theta,t)$:

$$\Delta\sigma(\lambda,\theta,t) = a\rho_w \sum_{n=1}^{n_{max}} \sum_{m=-n}^{n} T^{\sigma}_{nm}(t)\bar{Y}_{nm}(\lambda,\theta) \tag{1}$$

Here, ρ_w, is the density of seawater taken to be 1025 $\frac{kg}{m^3}$, and a denotes the Earth's radius. The 4π-normalized harmonic base functions, $\bar{Y}_{nm}(\lambda,\theta)$, are related to the associated Legendre functions[1] at colatitude θ and longitude λ as follows:

$$\bar{Y}_{nm}(\lambda,\theta) = \begin{cases} \bar{P}_{n|m|}(\cos\theta)\cos m\lambda, & m \geq 0 \\ \bar{P}_{n|m|}(\cos\theta)\sin m\lambda, & m < 0 \end{cases}$$

The three data sets used in this study, GRACE , GPS network solutions and modelled OBP, have three different relations with the unknown surface loading coefficients. The observation equations are explained in more detail in Rietbroek et al. (2009); Kusche and Schrama (2005), but we repeat them in the sections below, while adding some modifications. After the construction of the weekly normal equations we can

[1] no Condon-Shortley phase applied

combine and weigh the different data sets using their errors.

As a background model we use the weekly GRACE-GAC product, containing modelled atmospheric and oceanic signal from the ECWMF and the ocean model for circulation and tides (OMCT) respectively, which is restored after the inversion. Furthermore, in contrast to Rietbroek et al. (2009), the GPS data are added in the form of normal equations. This prohibits the propagation of possible numerical instabilities from the GPS-only error-covariance matrix.

2.2. GRACE weekly solutions

Parallel to the monthly EIGEN-GRACE05S time series of the GRACE Science Data System, GFZ has also processed weekly gravity field solutions. These models have a higher temporal resolution compared to the other processing centres and provide insight into mass variations which take place at ten-daily or even shorter time scales such as barotropic Rossby waves, continental water storage changes or solid Earth and ocean tides (Ilk et al., 2004). The weekly models have been derived from 7-day batches, aligned to the GPS calendar week, of daily GRACE normal equation systems using the same release 4 processing standards and background models as applied for the monthly solutions. With no further constraints applied, solutions up to degree and order 30 can be yielded. This was based on a dedicated ground track analysis based on GRACE orbit configuration and GRACE instrument data availability. Besides the pure also pseudo-weekly (smoothed version from combination with two down-weighted preceding and succeeding weekly products) solutions have been derived. Although the pure weekly solutions show a larger variability, they generally agree well with the monthly solutions (Flechtner et al., 2010). For some weeks, larger deviations ("outliers") are visible which do not necessarily correlate with the results of the ground track analysis. Therefore, it seems to be plausible that some of these outliers rather represent physically induced signal than noise. The well-known "GRACE C_{20} bias", e.g. when compared to the latest version of GFZ's release 4 LAGEOS time series (Flechtner et al., 2010), is obvious and has still to be investigated.

Within the inversion, weekly GRACE normal equations, are degree-wise calibrated (Rietbroek et al., 2009). The residual Stokes coefficients, $\delta\Phi_{nm}(t)$, can be linked to the surface loading coefficients by a diagonal design matrix having entries:

$$\delta\Phi_{nm}(t) = \frac{3\rho_w(1+k'_n)}{\rho_e(2n+1)} T^{\sigma}_{nm}(t) \tag{2}$$

The Earth's elastic response to surface loading is modelled using the spectral load Love numbers k'_n, l'_n, h'_n derived from the Preliminary Reference Earth Model (PREM) (Dziewonski, 1981).

During the GRACE processing, the orbits of the GPS satellites are fixed (i.e. the estimated gravity field does not affect the GPS satellite orbits). The underlying coordinate system of the GRACE normal system equations is therefore determined by the reference frame of the GPS satellite orbits. Additionally, since the GRACE twins and the GPS satellites orbit the center of common mass (CM) of the Earth, their (relative) range observations provide no information of degree 1 Stokes variations, which are zero per definition in this frame. The well known deficit of GRACE is that applying equation 2 gives rise to a rank defect in terms of T^{σ}_{1m}, as $1 + {k'_1}^{(CM)}$ equals zero in the CM frame (Blewitt and Clarke, 2003). Throughout this paper, the superscript $^{(CX)}$ of the degree 1 load Love numbers indicate in which reference frame it is defined.

2.3. Modelled Ocean Bottom Pressure

Ocean bottom pressure (OBP) is modelled globally using the finite element sea-ice ocean model (FESOM, Timmermann et al. (2009); Böning (2009)). It solves the primitive equations and uses the Boussinesq approximation. Conservation of mass is achieved by applying a correction after Greatbatch (1994); Böning et al. (2008). A tetrahedral grid with a horizontal resolution of 1.5° at the ocean surface is applied. The model is initialized with temperature and salinity from the World Ocean Atlas 2001 (WOA01) and simulates OBP from 1958 to 2008. The model simulation is forced by daily mean data sets of the NCAR/NCEP reanalysis (Kalnay et al., 1996). The mass budget includes precipitation and evaporation from the NCAR/NCEP reanalysis, whereas evaporation is computed from latent heat flux. River runoff is introduced into the model, using surface runoff derived from the land surface discharge model (LSDM) (Dill, 2008). To restrict global mean ocean mass variations to reasonable limits, a two year high pass filter is applied to the mass balance terms of the model (Böning et al., 2008). OBP anomalies are computed on weekly time scale for 2003 to 2008 (Brunnabend et al., 2010, submitted). These anomalies have already been used in the previous studies of Jansen et al. (2010) and Rietbroek et al. (2009). The error of modelled OBP has been estimated by comparing OBP derived from two model simulations using different atmospheric forcing data sets (Brunnabend et al., 2010, submitted). The alternative model simulation includes six hourly atmospheric parameters provided by the ECMWF, (ECMWF, 1995; Uppala et al., 2006). Weekly error maps of modelled OBP are computed by the weekly root mean square of the daily mean difference between the two model simulations. In this study, the mean weekly errors are introduced as diagonal matrixes into the inversion scheme. To be consistent with the other data sets the OBP difference w.r.t. the GRACE-GAC product is fed in the inversion.

Whereas Rietbroek et al. (2009) used the modelled OBP as pseudo observations of absolute pressure (expressed in equivalent water height), we now assume that the pressure values are residuals with respect to the instantaneous geoid augmented with an unknown model mass correction:

$$\begin{aligned}\delta P(\lambda, \theta, t) &= P(\lambda, \theta, t) - N(\lambda, \theta, t) \\ &\approx \Delta M_0 + a \sum_{n=1}^{n_{max}} \sum_{m=-n}^{n} \zeta_n T^{\sigma}_{nm} \bar{Y}_{nm}(\lambda, \theta)\end{aligned} \tag{3}$$

Here, P is the ocean bottom pressure change expressed in equivalent water height. The symbol δP is the bottom pressure anomaly w.r.t. the geoid, N. Furthermore, ΔM_0 denotes an uniform mass correction, which absorbs remaining mass discrepancies in the model's fresh water fluxes. The degree dependent factor, ζ_n, maps the surface loading coefficients to the instantaneous geoid, which is the reference surface used in the ocean model.

$$\zeta_n = 1 - \frac{3\rho_w(1 + k'_n)}{\rho_e(2n + 1)} \tag{4}$$

Although usually neglected, this factor has a small effect on the inversion. Starting with 0.8 for $n = 1$, ζ_n quickly approaches 1 (0.99 for degree 30). The approximation sign stems from the fact that we assume a bandlimited spectrum, up to n_{max}, for surface loading. Finally, in the inversion we have excluded shallow nodes with depths from 800 m and those which are located in the Mediterranean Sea.

2.4. GPS reprocessing solutions

When surface loading is applied to the Earth, resulting crustal deformation can be measured by a network of permanent GPS receivers. In this study we use dedicated weekly normal equations constructed according to the IGS reprocessing standards (Rülke et al., 2008; Fritsche et al., 2009, for more info on the reprocessing). In particular, higher-order ionospheric terms have been accounted for. Moreover, detailed investigations have been carried out concerning the impact of different solar radiation pressure models. Here, the empirical CODE radiation pressure model (Springer et al., 1999) has been applied as a reference model.

In terms of consistency, the main advantage of the reprocessing solution is that both station positions and satellite orbits are estimated simultaneously. Here, the related orbit parameters are removed from the GPS normal equation systems by implicitly solving them. Since the GPS satellites are known to circle the center of mass (CM) of the Earth, the underlying coordinate system is relative to this CM. However, a rank defect still exists in terms of orientation and additional constraints would be needed to remove this.

For studies of surface loading, it is more intuitive to study the GPS site displacements in the center of figure (CF) frame. Therefore we apply 2 additional steps to preprocess the GPS normal equation systems. Firstly, a weekly network transformation is introduced in the form of 7 unknown Helmert parameters, which represent a translation($\delta\vec{\tau}$) a rotation($\delta\vec{\epsilon}$) and a scale change(δs). Secondly, the introduced rank defects are compensated by constraining the station positions of 132 well-distributed core stations. The translation, rotation and scale of those core stations are constrained towards zero, such that the corresponding network approximates the CF frame. The 2 steps above are performed by adapting the original normal matrix, $\mathbf{N}$, with its corresponding right hand side, $\vec{b}$, yielding an updated normal equation system ($\mathbf{N}^*$,$\vec{b}^*$).

$$\mathbf{N}^* = \begin{bmatrix} \mathbf{N} + \mathbf{\Psi}_c & \mathbf{NB} \\ \mathbf{B}^T\mathbf{N} & \mathbf{B}^T\mathbf{NB} \end{bmatrix}, \quad \vec{b}^* = \begin{bmatrix} \vec{b} \\ \mathbf{B}^T\vec{b} \end{bmatrix} \tag{5}$$

The matrix $\mathbf{B}$ maps the Helmert transformation parameters to the n station position changes ($\delta\vec{x}$).

$$\delta\vec{x} = \mathbf{B} \begin{bmatrix} \delta\vec{\tau} \\ \delta s \\ \delta\vec{\epsilon} \end{bmatrix} = \begin{bmatrix} B_1 \\ \vdots \\ B_n \end{bmatrix} \begin{bmatrix} \delta\vec{\tau} \\ \delta s \\ \delta\vec{\epsilon} \end{bmatrix} \tag{6}$$

$$B_i = \begin{bmatrix} 1 & 0 & 0 & x_i & 0 & z_i & -y_i \\ 0 & 1 & 0 & y_i & -z_i & 0 & x_i \\ 0 & 0 & 1 & z_i & y_i & -x_i & 0 \end{bmatrix} \tag{7}$$

The second preprocessing step is performed by regularizing with the matrix $\mathbf{\Psi}_c$ over the core stations only (denoted by subscript $_c$).

$$\mathbf{\Psi}_c = \mathbf{B}_c \left(\mathbf{B}_c^T\mathbf{B}_c\right)^{-1} \mathbf{D}^{-1} \left(\mathbf{B}_c^T\mathbf{B}_c\right)^{-1} \mathbf{B}_c^T \tag{8}$$

The diagonal weight matrix, $\mathbf{D}$, determines the weight of the constraint. In this study we use standard deviations of 0.1 mm, $3\,\mu as$ and 0.01ppb for the translation, rotation and scale respectively. In summary, this procedure essentially keeps the same degrees of freedom in the normal equation systems but expresses the underlying coordinate system in the CF system, while frame inconsistencies can be absorbed by the Helmert parameters.

The background model used should be consistent with that of GRACE. We constructed a GPS-derived drifting reference frame, additionally solving for station discontinuities, for the period 2002-2009. The associated Earth orientation was accounted for by using the C04 EOP (Earth Orientation Parameters) series from the International Earth Rotation Service (IERS), which is consistent with the GRACE processing. As an addition to the background model, we have added the loading effect of the GRACE-GAC product and the equilibrium ocean pole tide (Desai, 2002) on the station positions.

At this stage, we have weekly GPS normal equation systems with 7 unknown Helmert parameters and unknown Cartesian site coordinates expressed in an approximate CF frame. In order to prepare the system for the joint inversion we need to 1), rotate the coordinate system in a local (up, north, east) frame using rotation matrix $\mathbf{R}^T$ and 2) apply loading theory to link surface loading to site deformations by means of matrix $\mathbf{D}$. These deformations, in upward (δh), east (δe) and northward (δn) direction, at the GPS sites are related to the unknown surface loading coefficients in the following way:

$$\begin{aligned}
\delta h(\lambda,\theta,t) &= \frac{3a\rho_w}{\rho_e}\sum_{n,m}\frac{h'_n}{2n+1}T^{\sigma}_{nm}(t)\bar{Y}_{nm}(\lambda,\theta) \\
\delta e(\lambda,\theta,t) &= \frac{3a\rho_w}{\rho_e\sin\theta}\sum_{n,m}\frac{l'_n}{2n+1}T^{\sigma}_{nm}(t)\frac{\partial\bar{Y}_{nm}(\lambda,\theta)}{\partial\lambda} \\
\delta n(\lambda,\theta,t) &= \frac{3a\rho_w}{\rho_e}\sum_{n,m}\frac{l'_n}{2n+1}T^{\sigma}_{nm}(t)\frac{\partial\bar{Y}_{nm}(\lambda,\theta)}{\partial\theta}
\end{aligned} \tag{9}$$

Steps 1 and 2 above may be applied to the updated normal equations system from eq. 5 without the need for an inversion.

$$\mathbf{N}^{\dagger} = \begin{bmatrix} \mathbf{D}^T\mathbf{R}^T\mathbf{N}^*_{pp}\mathbf{R}\mathbf{D} & \mathbf{N}^*_{ph}\mathbf{R}\mathbf{D} \\ \mathbf{D}^T\mathbf{R}^T\mathbf{N}^*_{hp} & \mathbf{N}^*_{hh} \end{bmatrix}, \quad \vec{b}^{\dagger} = \begin{bmatrix} \mathbf{D}^T\mathbf{R}^T\vec{b}^*_p \\ \vec{b}^*_h \end{bmatrix} \tag{10}$$

The system is partitioned in blocks representing Cartesian positions and Helmert parameters denoted by the subscripts $_p$ and $_h$ respectively.

Since we have previously constrained the site deformations to an (approximate) CF frame it is important that appropriate degree 1 CF load Love numbers are selected in eq. 9. Those are obtained by applying the isomorphic frame transformations from Blewitt and Clarke (2003). Here, $h_1'^{(CF)}$, $l_1'^{(CF)}$ and $k_1'^{(CF)}$ have values -0.260, 0.130 and 0.026 respectively. Consequently, a large part of the network translation is now absorbed by T^{σ}_{1m}. At this stage, the Helmert parameters in eq. 9 should therefore be considered as residuals and their estimates are ideally close to zero (see results in sec. 3.2).

3. Results

3.1. Geocenter motion

The degree-1 surface loading coefficients from the inversion are related to the so-called geocenter motion. From a reference frame of choice, the center of mass of the Earth system ("the geocenter“) moves according to (Blewitt and Clarke, 2003):

$$\begin{bmatrix} r_x \\ r_y \\ r_z \end{bmatrix}^{(CX)} = (1 + k_1'^{(CX)})a\sqrt{3}\frac{\rho_w}{\rho_e}\begin{bmatrix} T^{\sigma}_{11} \\ T^{\sigma}_{1-1} \\ T^{\sigma}_{10} \end{bmatrix} \tag{11}$$

In contrast to the degree 1 load Love number used in the GPS observation equations (cf. eq. 9), we are allowed to choose one expressed in a different frame: $k_1'^{(CX)}$. It is convenient to use the frame associated with the center of mass of the solid Earth (CE), with $k_1'^{(CE)} = 0$, as it closely (within 3%) coincides with the CF frame and is independent of the used Earth model. This choice, which we apply in this study, results in a geocenter motion vector defined as the offset between the origins of the CM and CE frames.

Figure 1 shows the surface load induced geocenter motion in Cartesian coordinates. Annual and semi annual fits and the RMS of the series, after removing the seasonal fit, are provided in table 1. The joint inversion series generally match those of Rietbroek et al. (2009), although difference in the seasonal signal can be found, most notably in the Y and Z component. The main advantage of the reprocessing becomes clear from the RMS of the residual series. Here we find a RMS reduction of 0.5, 1.3 and 1.1 mm for the non-seasonal signal of the X, Y and Z components, respectively. Compared to the joint inversion, the GPS-only variations are larger, which is primarily caused by the lack of data over the ocean and at high latitudes.

In order to investigate the effect of the applied solar radiation pressure model we have constructed two GPS solution sets using the (older) physical ROCK models (Fliegel et al., 1992; Fliegel and Gallini, 1996) and the (newer) empirical CODE model. From the resulting normal equation systems we have estimated two sets of GPS-only load induced geocenter motion and two sets of joint inversion derived geocenter motion. The influence of the radiation pressure model on the joint inversion results appears to be marginal. The annual Z component of the geocenter motion increases by 0.8 mm and its phase shifts forward by 13 days, when using the CODE model. The differences can however not explain the larger discrepancy with the older series from Rietbroek et al. (2009). Other factors, arising from the reprocessing strategy and the difference in OBP weighting may have a larger influence. The Z component from the GPS-only series benefits from the used CODE model, in particular the annual signal shows an improved agreement with the joint inversion solutions. It is less clear how the X and Y components benefit from the used radiation pressure model. The difference is smaller than for the Z component, although the annual behavior for the ROCK derived series is in better agreement with the joint inversion series.

It is illustrative to plot direction and magnitude of $\vec{r}$ to obtain an idea of which areas are most influenced by the geocenter motion (figure 2). In addition, the seasonal (annual + semi annual) fits are shown as well. The track of the seasonal geocenter and its antipode crosses some important hydrological areas: the Amazon, Australia, central Asia and Europe. The maximum magnitude is in the order of 4,4 mm, which indicates that neglecting the geocenter motion in those areas may have negative side-effects when comparing space based measurements with terrestrial measurements. In terms of equivalent water heights, the additional amplification by $\frac{\rho_e}{\rho_w} \approx 5.4$ causes variations in the order of a couple of centimeters.

3.2. *Estimated Helmert parameters*

The estimated Helmert parameters are small but not negligible (see figure 3). The translation parameters, representing the non-surface loading induced network shift, stay below the mm level. The scale and rotation serve as corrections to adjust the GPS to the GRACE (and OBP) data. The largest impact comes from the estimated scale parameter. In terms of station displacement, GPS stations will be affected by a maximum of 3 mm radial shift. There is no physical justification for this seasonal inflation and deflation of the GPS network, but such phenomena can arise from GPS technique errors such as residuals induced by a mismodelling of the tropospheric path delay (Heflin et al., 2002). Since we estimate surface loading simultaneously and in a combination with GRACE, aliasing of this signal in combination with a non-perfect GPS network (Lavallée et al., 2006) seems unlikely. We find that the radiation pressure models (ROCK versus CODE), used within the different GPS processing series, affect the estimated scales, but can not explain the remaining variability. Changing the radiation pressure model causes a shift of the seasonal signal (0.24 ppb amplitude, 0.2 ppb RMS) of about 24 days.

3.3. *Global in-situ BPR comparison*

We have compared the joint inversion results with ground truth data from ocean bottom pressure recorders (BPRs) from the AWI database (Macrander et al., 2010). The BPR data have been detided and averaged over the GPS weeks, to make them equivalent in the time domain. It has been shown by Böning et al. (2008) that the spatial extent of the correlation of ocean signal around recorders is large. This suggests that the BPRs should pick up a considerable part of large scale signals, which fall also into the spectrum of the joint inversion solutions. During the research for this paper we have found that a slight smoothing of the joint inversion results increased the BPR correlations. We therefore use a modified joint inversion solution for the comparison with BPRs. The actual smoothing of the joint inversion solution is implemented as an increase of the FESOM OBP weight by a factor of 1/3.3 in terms of standard deviation. This effectively constraints the joint inversion solution towards the FESOM model, without compromising the total ocean content (a uniform OBP correction is still estimated).

Figure 4 (left) shows the correlation of the in-situ timeseries with the joint inversion solution. Overall correlations are positive (0.51), but the agreement is dependent on the region. The strongest correlations, are found in the Framstrait, the South Atlantic and the South Indian ocean, where the OBP signal is large.

In addition, we assessed the correlation of the non-seasonal signal (figure 4, right) by removing a seasonal fit from the BPR and inversion timeseries and calculate again the correlation. On average and considering only BPRs with time series longer than a year, this procedure reduces the RMS by around 30% to 1.6 cm for the inversion series. A smaller reduction of 15% resulting in a RMS of 3.8 cm is observed for the insitu series. Furthermore, we find an averaged fitted annual amplitude of 1.8 cm for the inversion and 2.1 cm for the recorders. It should be stressed that neglecting the degree 1 coefficients decreases the overall correlation to 0.41. Compared to the results of Macrander et al. (2010) we find all positive correlations in the Drake passage and in the Atlantic MOVE array (Kanzow et al., 2005), which is most likely due to the contribution of FESOM OBP data in the inversion. However, a direct comparison remains difficult due to the different smoothness and time resolution of the solutions.

3.4. GPS station residuals

To see how much of the GPS site deformation signal can be explained by surface loading, we have constructed and compared two versions of station displacement timeseries. The first version is directly derived from the GPS-only normal equation, without an a priori loading model. The second version uses our inversion results as an a priori loading model. The station residuals from the second version should have therefore a significant part of their surface loading signal removed.

The reduction in RMS of the estimated station displacement with and without the a priori inversion results are plotted in figure 5 (left). Only 8 stations show an increase in their RMS, indicating other more dominant effects are at play at the sites. The 'worst' station, NSSP, shows a RMS increase of 10%, which is small in comparison to the RMS reductions seen for the other stations (e. g. 54% for LAMA).

The surface loading signal is expected to be most prominent in the height component on a seasonal scale. We fitted a seasonal curve to the station height component for both versions (with and without the a priori loading model) and compared the amplitudes (figure 5, right). From the 189 stations considered, 10 stations have a fitted seasonal signal considered insignificant at the 98% confidence level. From the significant stations 15 stations show an actual increase of at least 10% in the annual amplitude with the a priori loading model. On the other hand, the majority (151) of the stations have reductions in amplitude of at least 10%.

4. Conclusion

We have constructed weekly surface loading estimates by combining data from GRACE gravimetry, surface deformation from reprocessed GPS observations and modelled ocean bottom pressure. This strategy has the advantages that the geocenter motion can be estimated simultaneously, correlated errors from GRACE decrease and that mass correction parameters can be estimated for the ocean model.

The benefit from using the reprocessing GPS solution is twofold. Firstly, the GPS normal equations are constructed in a more physically consistent sense by estimating station and satellite positions simultaneously in the center of mass system. Secondly, the consistent reprocessing over the whole period yields more accurate and consistent station deformations.

In comparison with Rietbroek et al. (2009), who used the IGS GPS solutions, we find a smoother geocenter motion and smaller variations in the estimated Helmert parameters. GPS derived parameter estimates are still affected by systematic modelling deficiencies, as is apparent from the variation in the scale parameter, which can constitute up to 3 mm of the receiver displacement. We find that changing the radiation pressure model used in the GPS processing has only a marginal influence on the estimated geocenter motion and Helmert parameters, in contrast with a GPS only inversion where the Z component strongly benefits from using the newer CODE model (vs. the older ROCK models). This pleads for the robustness of the joint inversion method we apply.

In future studies, we may choose an alternative GPS processing strategy by skipping the steps from eq. 5 and using the degree 1 load Love numbers of the CM frame in eq. 9. However, since no separate Helmert parameters are estimated in that case, care must be taken that scale variations do not erroneously propagate into our surface loading estimates.

Overall correlations with timeseries of in-situ bottom pressure recorders are good (weighted correlation of 0.51), with the strongest correlations found at the higher latitudes. After removing a seasonal fit to the series we still find an overall correlation of 0.45, indicating that the solution picks up a significant part of oceanic subseasonal signal. Furthermore, degree 1 surface loading variations play an important role since their neglection cause a decrease in correlation to 0.41.

Using our inversion results as an a priori model in the GPS normal equations yields station timeseries with a reduced RMS and smaller annual height component, although some (8 in terms of RMS and 15 in terms of annual height component) outliers remain. In contrast to the findings of van Dam et al. (2007), we find a more consistent behavior of the GPS stations over Europe. The local disagreements in annual signal found by van Dam et al. (2007) were attributed mostly to GPS technique errors, which appear to be smaller in this study due to the reprocessing strategy. Considering the above, our inversion results are an attractive data set to reduce the (seasonal) surface loading signal in the GPS stations.

Acknowledgments

We would like to thank the German Space Operations Center (GSOC) of the German Aerospace Center (DLR) for providing continuously and nearly 100% of the raw telemetry data of the twin GRACE satellites. The authors acknowledge support provided by the German Research Foundation under grants KU 1207/6-1, FL 592/1-1, SCHR 779/4-1, and DI 473/41-2 within the Special Priority Program SPP 1257 Mass Transport and Mass Distribution in the System Earth. We thank two anonymous reviewers for their efforts and the constructive feedback on this paper.

References

Blewitt, G., Clarke, P., 2003. Inversion of earth's changing shape to weigh sea level in static equilibrium with surface mass redistribution. Journal of Geophysical Research (Solid Earth) 108, 2311.

Blewitt, G., Lavallée, D., Clarke, P., Nurutdinov, K., 2001. A new global mode of earth deformation: seasonal cycle detected. Science 294, 2342–5.

Böning, C., 2009. Validation of ocean mass variability derived from the Gravity Recovery and Climate Experiment - Studies utilizing in-situ observations and results from a Finite Element Sea-ice Ocean Model. Ph.D. thesis. University of Bremen, Germany.

Böning, C., Timmermann, R., Macrander, A., Schröter, J., 2008. A pattern-filtering method for the determination of ocean bottom pressure anomalies from grace solutions. Geophysical Research Letters 35, L18611.

Brunnabend, S.E., Rietbroek, R., Timmermann, R., Schröter, J., Kusche, J., 2010. Improving grace analysis by modelling ocean bottom pressure uncertainty. submitted to Journal of Geophysical Research .

Chen, J.L., Rodell, M., Wilson, C.R., Famiglietti, J.S., 2005. Low degree spherical harmonic influences on gravity recovery and climate experiment (grace) water storage estimates. Geophysical Research Letters 32, 14405.

van Dam, T., Wahr, J., Lavallée, D., 2007. A comparison of annual vertical crustal displacements from gps and gravity recovery and climate experiment (grace) over europe. Journal of Geophysical Research 112, B03404.

Desai, S.D., 2002. Observing the pole tide with satellite altimetry. Journal of Geophysical Research 107, 3186.

Dill, R., 2008. Hydrological model LSDM for operational earth rotation and gravity field variations. Scientific Technical Report; 08/09. Helmholtz-Zentrum Potsdam Deutsches GeoForschungsZentrum.

Dong, D., 2003. Origin of the international terrestrial reference frame. Journal of Geophysical Research 108, 2200.

Dziewonski, A., 1981. Preliminary reference earth model. Physics of The Earth and Planetary Interiors 25, 297.

ECMWF, 1995. The description of the ecmwf/wcrp level iii-a global atmospheric data archive.

Flechtner, F., Dahle, C., Neumayer, K.H., König, R., Förste, C., 2010. The release 04 champ and grace eigen gravity field models. System Earth via Geodetic-Geophysical Space Techniques, Adv. Technologies in Earth Sciences , 41.

Fliegel, H.F., Gallini, T.E., 1996. Solar force modeling of block iir global positioning system satellites. Journal of Spacecraft and Rockets 33, 863.

Fliegel, H.F., Gallini, T.E., Swift, E.R., 1992. Global positioning system radiation force model for geodetic applications. Journal of Geophysical Research 97, 559.

Fritsche, M., Dietrich, R., Rülke, A., Rothacher, M., Steigenberger, P., 2009. Low-degree earth deformation from reprocessed gps observations. GPS Solutions 14, 165.

Greatbatch, R.J., 1994. A note on the representation of steric sea level in models that conserve volume rather than mass. Journal of Geophysical Research 99, 12767.

Heflin, M., Argus, D., Jefferson, D., Webb, F., Zumberge, J., 2002. Comparison of a gps-defined global reference frame with itrf2000. GPS Solutions 6, 72–75. 10.1007/s10291-002-0015-5.

Heflin, M., Watkins, M., 1999. Geocenter estimates from the global positioning system, in: IERS Analysis Campaign to Investigate Motions of the Geocenter. Obs. de Paris, Paris. chapter IERS Technical Note No.25, pp. 55–70.

Ilk, K.H., Flury, J., Rummel, R., Schwintzer, P., Bosch, W., Haas, C., Schröter, J., Stammer, D., Zahel, W., Miller, H., Dietrich, R., Huybrechts, R., Schmeling, H., Wolf, D., Riegger, J., Bardossy, A., Güntner, A., 2004. Mass transport and mass distribution in the earth system : Contribution of the new generation of satellite gravity and altimetry missions to geosciences. Proposal for a German Priority Research Program .

Jansen, M.J.F., Gunter, B.C., Kusche, J., 2009. The impact of grace, gps and obp data on estimates of global mass redistribution. Geophysical Journal International 177, 1.

Jansen, M.J.F., Gunter, B.C., Rietbroek, R., Dahle, C., Kusche, J., Flechtner, F., Brunnabend, S.E., Schröter, J.., 2010. Estimating sub-monthly global mass transport signals using grace, gps and obp data sets, in: Mertikas, S. (Ed.), Proc. of the IAG International Symposium on Gravity, Geoid and Earth Observation (GGEO2008), Chania, Crete, June 23-27, 2008, Springer. pp. 587–593.

Kalnay, E., Kanamitsu, M., Kistler, R., Collins, W., Deaven, D., Gandin, L., Iredell, M., Saha, S., White, G., Woollen, J., Zhu, Y., Leetmaa, A., Reynolds, R., Chelliah, M., Ebisuzaki, W., Higgins, W., Janowiak, J., Mo, K.C., Ropelewski, C., Wang, J., Jenne, R., Joseph, D., 1996. The ncep/ncar 40-year reanalysis project. Bulletin of the American Meteorological Society 77, 437–471.

Kanzow, T., Flechtner, F., Chave, A., Schmidt, R., Schwintzer, P., Send, U., 2005. Seasonal variation of ocean bottom pressure derived from gravity recovery and climate experiment (grace): Local validation and global patterns. Journal of Geophysical Research 110.

Kusche, J., Schrama, E.J.O., 2005. Surface mass redistribution inversion from global gps deformation and gravity recovery and climate experiment (grace) gravity data. Journal of Geophysical Research (Solid Earth) 110, 9409.

Lavallée, D.A., van Dam, T., Blewitt, G., Clarke, P.J., 2006. Geocenter motions from gps: A unified observation model. Journal of Geophysical Research 111, B05405.

Macrander, A., Böning, C., Boebel, O., Schröter, J., 2010. Validation of grace gravity fields by in-situ data of ocean bottom pressure, in: Stroink, L., Mosbrugger, V., Wefer, G., Flechtner, F.M., Gruber, T., Güntner, A., Mandea, M., Rothacher, M., Schöne, T., Wickert, J. (Eds.), System Earth via Geodetic-Geophysical Space Techniques. Springer Berlin Heidelberg. chapter Advanced Technologies in Earth Sciences, pp. 169–185.

Rietbroek, R., Brunnabend, S., Dahle, C., Kusche, J., Flechtner, F., Schröter, J., Timmermann, R., 2009. Changes in total ocean mass derived from grace, gps, and ocean modeling with weekly resolution. Journal Of Geophysical Research-Oceans 114, C11004.

Rülke, A., Dietrich, R., Fritsche, M., Rothacher, M., Steigenberger, P., 2008. Realization of the terrestrial reference system by a reprocessed global gps network. J. Geophys. Res. 113.

Springer, T.A., Beutler, G., Rothacher, M., 1999. A new solar radiation pressure model for gps. Advances in Space Research 23, 673.

Tapley, B.D., Bettadpur, S., Ries, J.C., Thompson, P.F., Watkins, M.M., 2004. Grace measurements of mass variability in the earth system. Science 305, 503–506.

Timmermann, R., Danilov, S., Schröter, J., Böning, C., Sidorenko, D., Rollenhagen, K., 2009. Ocean circulation and sea ice distribution in a finite element global sea ice-ocean model. Ocean Modelling 27, 114–129.

Uppala, S.M., Kållberg, P.W., Simmons, A.J., Andrae, U., Bechtold, V.D.C., Fiorino, M., Gibson, J.K., Haseler, J., Hernandez, A., Kelly, G.A., Li, X., Onogi, K., Saarinen, S., Sokka, N., Allan, R.P., Andersson, E., Arpe, K., Balmaseda, M.A., Beljaars, A.C.M., Berg, L.V.D., Bidlot, J., Bormann, N., Caires, S., Chevallier, F., Dethof, A., Dragosavac, M., Fisher, M., Fuentes, M., Hagemann, S., Hólm, E., Hoskins, B.J., Isaksen, L., Janssen, P.A.E.M., Jenne, R., Mcnally, A.P., Mahfouf, J.F., Morcrette, J.J., Rayner, N.A., Saunders, R.W., Simon, P., Sterl, A., Trenberth, K.E., Untch, A., Vasiljevic, D., Viterbo, P., Woollen, J., 2006. The era-40 re-analysis. Quarterly Journal of the Royal Meteorological Society 131, 2961.

Wu, X., Argus, D.F., Heflin, M.B., Ivins, E.R., Webb, F.H., 2002. Site distribution and aliasing effects in the inversion for load coefficients and geocenter motion from gps data. Geophysical Research Letters 29, 2210.

Wu, X., Heflin, M.B., Ivins, E.R., Fukumori, I., 2006. Seasonal and interannual global surface mass variations from multisatellite geodetic data. Journal of Geophysical Research (Solid Earth) 111, 9401.

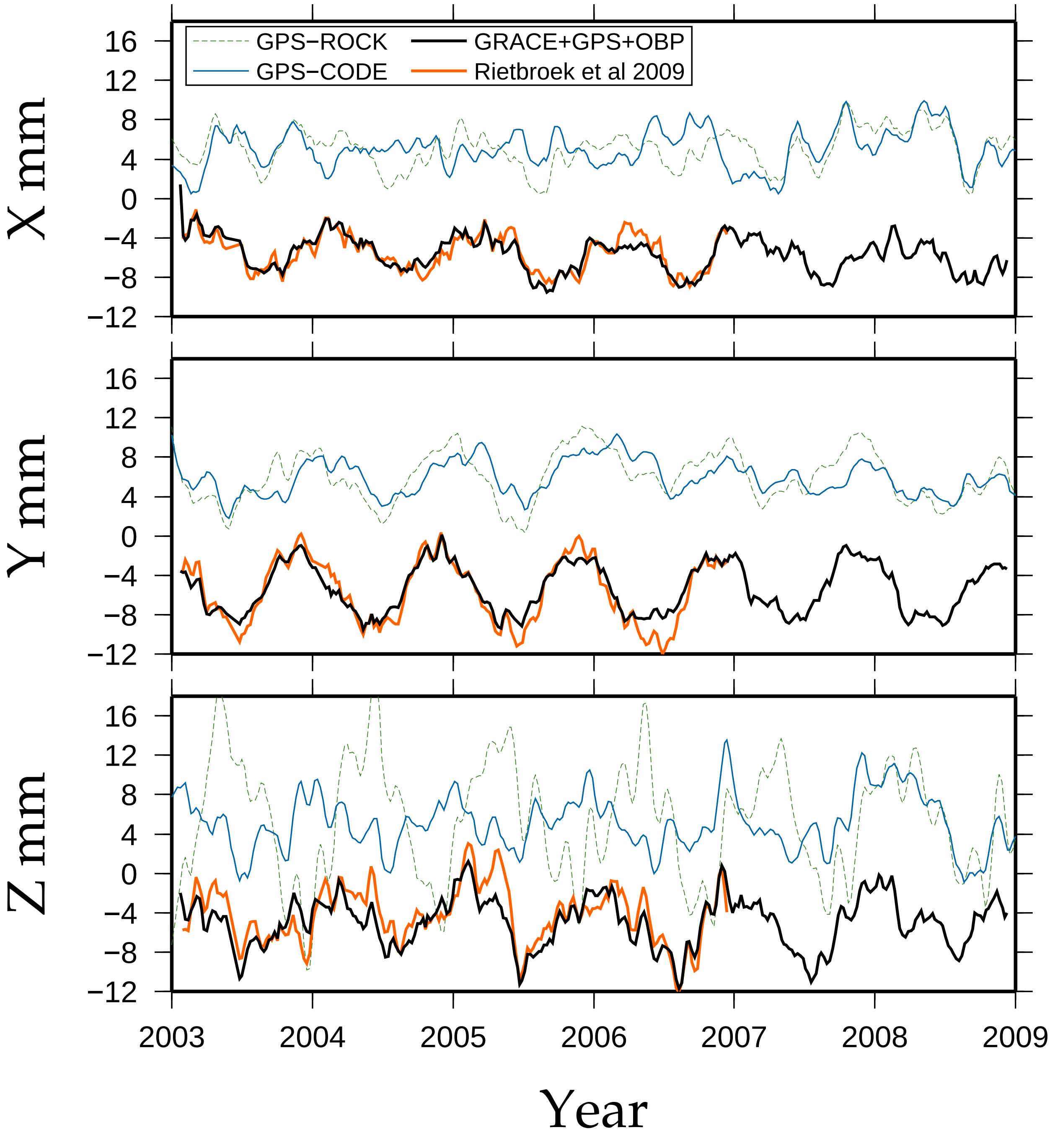

Figure 1: Surface load induced geocenter motion seen from the CE frame for: 1) GPS only estimates with the ROCK and CODE radiation pressure models applied (Fritsche et al., 2009) and 2) Joint inversion estimates from a previous study by Rietbroek et al. (2009) and the current combination solution. The GPS-only and joint inversion curves are shifted by +5 mm and -5 mm respectively for clarity. Additionally, a 1 month running mean was applied to the series.

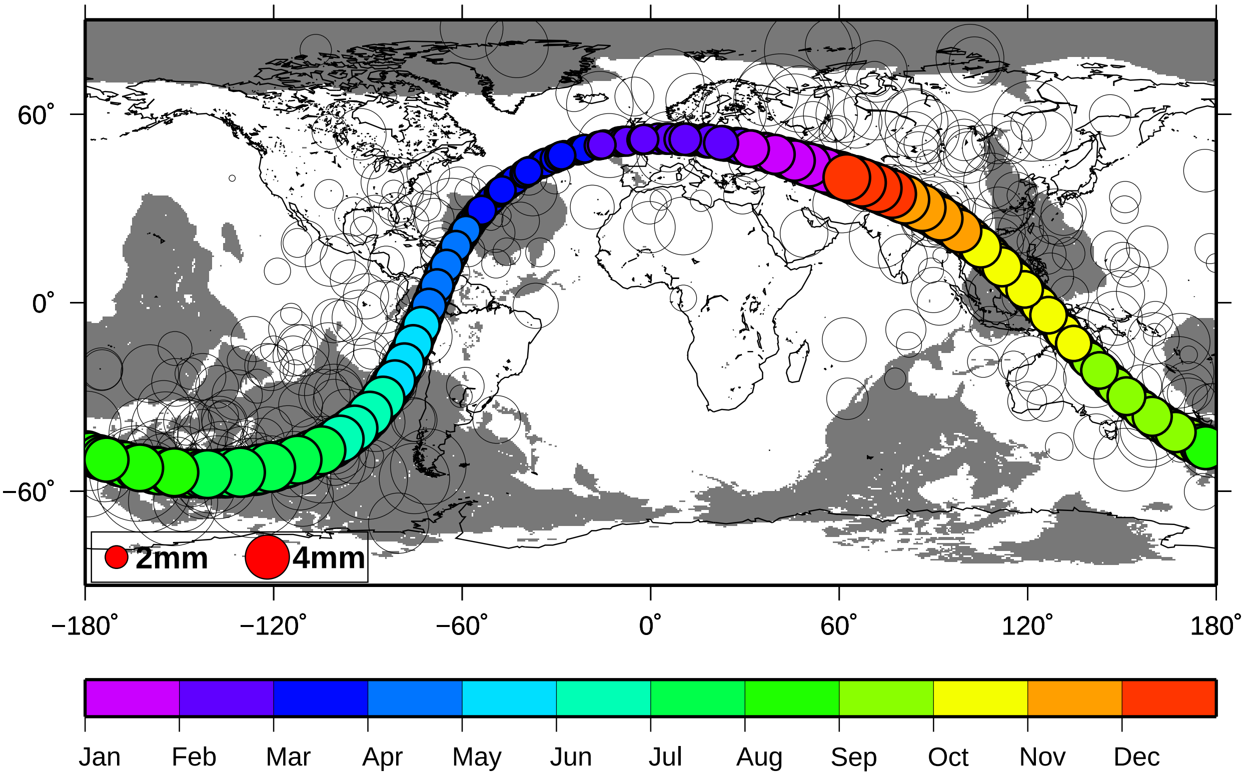

Figure 2: Direction and magnitude of the estimated geocenter motion. The colored circles represent the seasonal (annual+ semiannual) fit to te geocenter, with the color denoting the phase in months. Transparent circles denote the weekly geocenter values. Also affected, but in an inverse sense, are the locations at the antipodes (in gray).

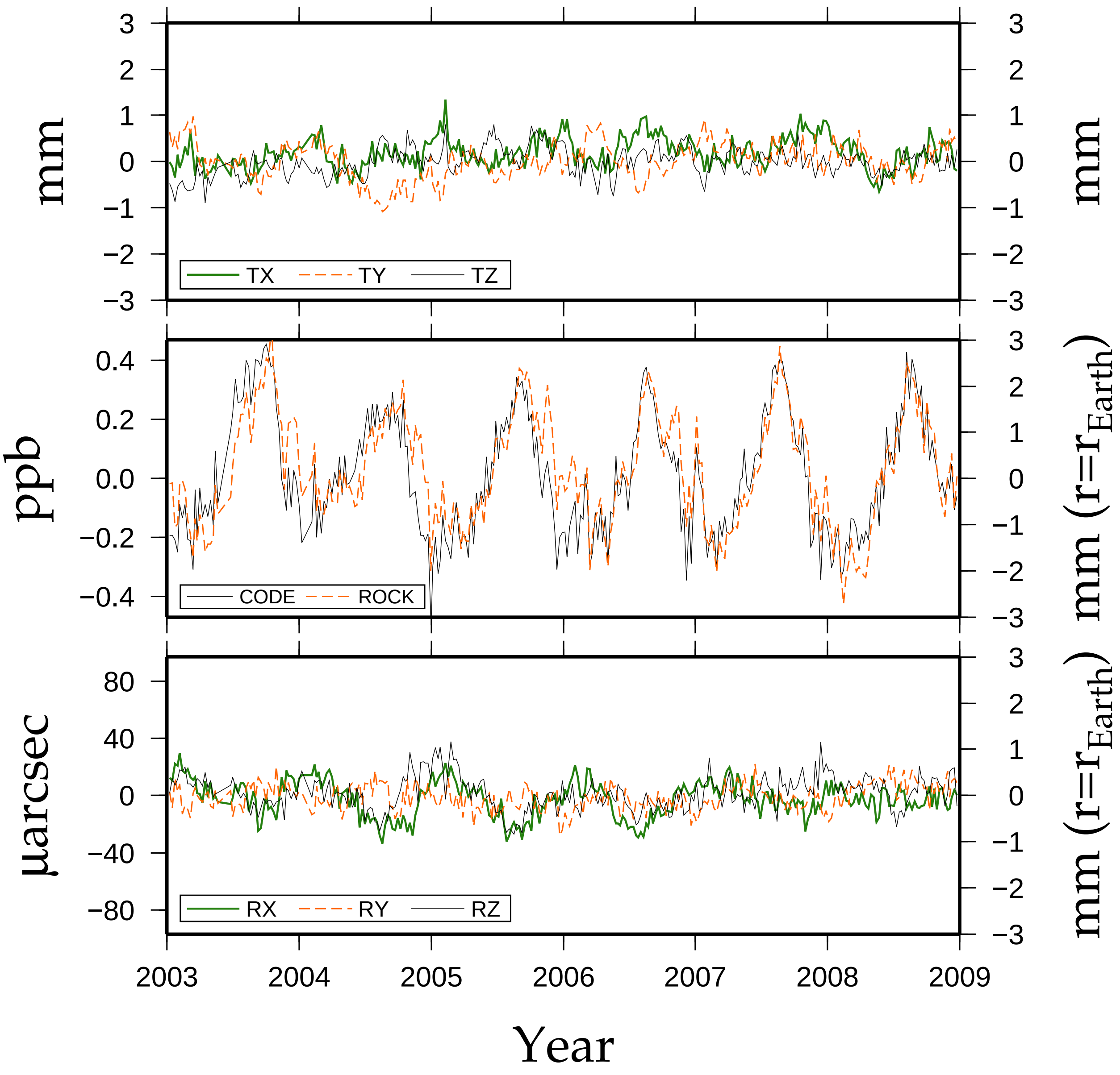

Figure 3: Estimated Helmert parameters: translation, scale and rotation derived from the joint inversion. The translation represent that part of the GPS network shift (w.r.t. CM) which is not induced by surface loading. The scale and rotation mostly absorb technique errors in the GPS processing and are constrained by the addition of GRACE and OBP data. The right axis spans the corresponding network displacement in mm at the Earth's surface. In the scale subplot, the estimated scale from the joint inversion, using the ROCK models in the GPS processing, is additionally plotted. The influence of the ROCK models on the translation and rotation is smaller and is not plotted.

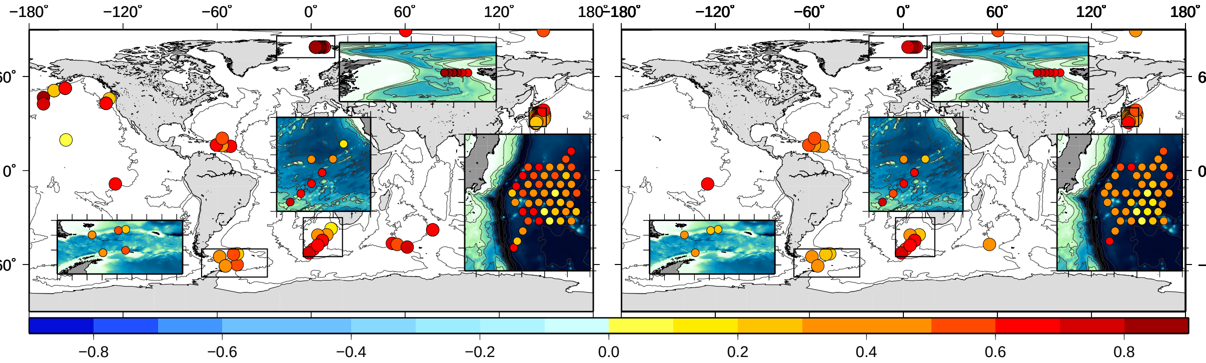

Figure 4: Correlations of the joint inversion solution with detided in-situ BPR time series from the AWI database. The bathymetry contour of 4000 m is given in gray. Regions with dense BPR arrays are magnified with bathymetry as background. The left and right panel show the correlations with and without the seasonal signal. For the seasonal fit, only stations with a continuous local time series of at least 1 year are plotted. The weighted overall correlation is 0.51 for the full BPR series and 0.45 for the reduced series.

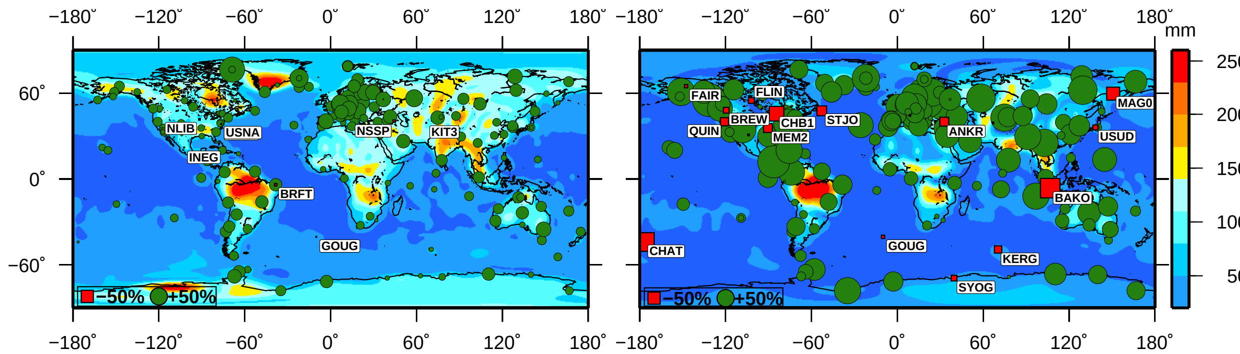

Figure 5: Left: Reduction in the RMS of GPS station displacements when using the joint inversion results as an a priori model. Large green circles show a strong decrease of the GPS time series while red squares with station tags show a RMS increase when using the inversion results. Color image beneath the circles denote the RMS of the joint inversion solution. Maximum RMS increase is 10% for NSSP while the maximum RMS reduction is 54% (LAMA), excluding the sparsely sampled THU1 (73%). Right: Reduction in fitted seasonal amplitude of the height component of stations with a seasonal signal which is significant at the 98% level. The color image beneath the stations represents the seasonal amplitude of the joint inversion. For clarity, stations with an increase of at least 10% are provided with a name tag. Maximum increase found is 82% for BAKO, maximum amplitude reduction is 99% for station AIS1.

	X					Y					Z				
	Annual		Semiann.		RMS	Annual		Semiann.		RMS	Annual		Semiann.		RMS
	Am.	ph.	Am.	ph.	post.	Am.	ph.	Am.	ph.	post.	Am.	ph.	Am.	ph.	post.
This study (CODE)	2.1	56	0.6	162	1.4	3.4	327	0.2	121	0.9	3.0	18	0.6	126	1.9
This study (ROCK)	2.0	63	0.5	160	1.4	3.4	326	0.2	124	0.9	2.2	31	0.6	117	2.2
Rietbroek et al. (2009)	2.2	75	0.3	142	1.9	4.6	335	0.4	104	2.2	2.6	64	1.4	106	3.0
GPS only (CODE)	0.9	182	0.7	137	2.4	1.7	2	0.3	163	2.5	2.5	17	0.6	172	3.2
GPS only (ROCK)	1.5	43	0.8	139	2.2	3.1	331	0.3	162	2.7	5.7	126	0.9	131	5.7

Table 1: Seasonal fits, in mm amplitude and phase in doy and posteriori RMS (mm) of geocenter motion time series for the following solutions: 1) Joint inversion (GRACE+GPS+OBP) with GPS data using the CODE radiation pressure model, 2) as 1 but using the ROCK radiation pressure models, 3) Time series from Rietbroek et al. (2009) (with corrected semiannual phase), 4) GPS only derived series using the CODE model (Fritsche et al., 2009), 5) as 4 but with the ROCK models.